JOURNAL OF GUIDANCE, CONTROL, AND DYNAMICS
Vol. 17, No. 3, May–June 1994

Optimal Multiple-Impulse Satellite Evasive Maneuvers

John E. Prussing*
University of Illinois at Urbana-Champaign, Urbana, Illinois 61801
and
Ronald S. Clifton†
The Aerospace Corporation, El Segundo, California 90245

Minimum-fuel, impulsive solutions are obtained for the evasive maneuver of a satellite followed by a rendezvous with the original orbit station. The evasion distance and time are constrained. Both free and constrained final time cases are considered. Primer vector theory is used to obtain optimal solutions, which include three-impulse solutions for an arbitrarily oriented evasion radius vector of a specified magnitude, and two-impulse free-return trajectories for certain specific evasion radius vectors. On some three-impulse solutions the primer vector indicates that the addition of a fourth impulse to the return trajectory will lower the fuel cost.

Nomenclature

A = 3×3 coefficient matrix in CW equations, Eq. (2)
$\boldsymbol{B}$ = 3×3 coefficient matrix in CW equations, Eq. (3)
D = determinant of the matrix N, Eq. (A6)
H = Hamiltonian function, Eq. (B9)
J = velocity-change cost of nominal three-impulse trajectory
K = time interval between initial and midcourse impulse, $t_m - t_o$
L = time interval between final and midcourse impulse, $t_f - t_m$
$\boldsymbol{M}$ = 3×3 partition of state transition matrix, Eq. (4)
$\boldsymbol{N}$ = 3×3 partition of state transition matrix, Eq. (4)
n = mean motion in nominal circular reference orbit
$\boldsymbol{p}$ = primer vector
p = magnitude of primer vector
$\boldsymbol{Q}$ = matrix defined in Eq. (20)
R = radius of threat sphere
$\boldsymbol{r}$ = relative position vector
$\boldsymbol{S}$ = 3×3 partition of state transition matrix, Eq. (4)
s = reference time
$\boldsymbol{T}$ = 3×3 partition of state transition matrix, Eq. (4)
T_R = maximum allowed evasion time
t = time
u = $\theta/2$, Eq. (A7)
$\boldsymbol{v}$ = relative velocity vector
w = scalar defined after Eq. (40)
$\boldsymbol{x}$ = relative position velocity state vector
x = radial relative position coordinate, Fig. (1)
y = tangential relative position coordinate, Fig. (1)
Z = factor in determinant D, Eq. (A7)
z = out-of-plane relative position coordinate, Fig. (1)
α = $3\tau^*/4$, Eq. (36)
$\Delta \boldsymbol{v}$ = vector velocity change due to thrust impulse
Δv = magnitude of vector velocity change due to thrust impulse
θ = elapsed time since a reference time, $t - s$
π_m = discontinuity in the out-of-plane midcourse primer rate, Eq. (42b)
τ = time interval between initial and final impulse, $t_f - t_o$
τ^* = time interval between initial and final impulse on a free-return trajectory
Φ = 6×6 state transition matrix
ϕ = angle between the midcourse position vector $\boldsymbol{r}_m$ and the x axis
$\boldsymbol{0}$ = zero vector
$(\dot{*})$ = time derivative of $(*)$, $d(*)/dt$

Subscripts

f = final impulse
k = generic subscript that may be o, m, or f
m = midcourse impulse
o = initial impulse
tot = total
x = x component
y = y component
z = z component

Superscripts

T = transpose of a vector or matrix
$-$ = immediately before thrust impulse
$+$ = immediately after thrust impulse
-1 = inverse of a matrix

Received June 7, 1990; revision received July 23, 1993; accepted for publication July 26, 1993. Copyright © 1993 by the American Institute of Aeronautics and Astronautics, Inc. All rights reserved.

*Professor, Department of Aeronautical and Astronautical Engineering. Fellow AIAA.

†Senior Member of Technical Staff, Astrodynamics Department. Member AIAA.

Introduction

IN the operational lifetime of a satellite, it may be necessary to perform avoidance or evasive maneuvers for the satellite to survive. A maneuver that is often considered is simply to remove the satellite from its station on orbit using onboard thrusters to a safe location. Following this, the satellite may either establish a new orbit that shares some of the desirable characteristics of the original orbit, return to a new station on the original orbit, or return to the original station on the original orbit. It is this last "return-on-station" option that is considered in this article, because it is the most demanding, but also it completely re-establishes the original satellite configuration.

The objective of this study is to determine minimum-fuel strategies for return-on-station maneuvers for both constrained and open final times. Fuel expenditure is critical because the operational lifetime of the satellite is greatly influenced by its ability to maneuver, which in turn is greatly affected by the fuel consumption of previous maneuvers.

The literature on optimal avoidance or evasive maneuvers is quite limited. Kelley et al. have investigated various aspects of the problem in Refs. 1 and 2. The approach used in the present study is to apply primer vector theory to obtain minimum-fuel solutions. This theory has been successfully applied in several impulsive rendezvous and intercept applications, such as Refs. 3 and 4. The return-on-station maneuver that is analyzed is essentially a rendezvous problem with an interior point constraint representing the safe intermediate location of the satellite. Preliminary results for the nonlinear version of this problem were obtained by Clifton.[5]

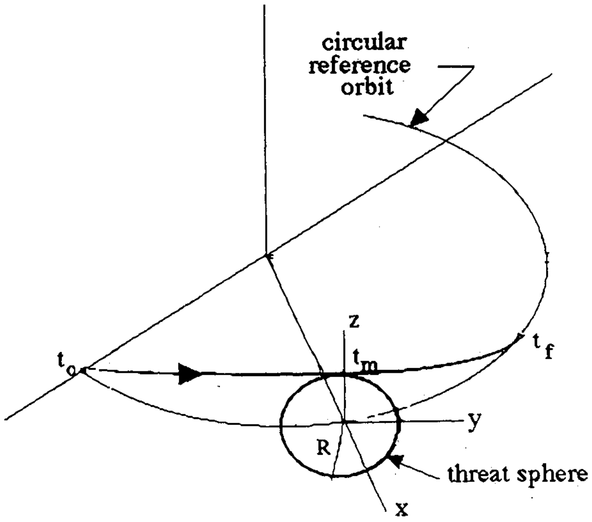

Fig. 1 Reference orbit and local vertical *xyz* coordinate frame.

The present study of the linearized approximation, which is valid because the evasion distance is small compared with the satellite orbital radius, provides more insight from the analytical solutions that are available. Other recent related studies are Refs. 6–9.

Linear Dynamic Model

For an Earth-orbiting satellite, an avoidance maneuver to a distance of 200 km from the original orbit station represents a 3% deviation relative to the nominal orbital radius for low-Earth orbit (LEO). For geosynchronous Earth orbit (GEO), 850 km is less than 2%. For this reason a linearized analysis using the Hill-Clohessy-Wiltshire (CW) equations[10,11] is justified.

The CW equations describe the motion of a satellite relative to a point on a circular reference orbit. The coordinate frame employed as shown in Fig. 1 is a rotating local vertical frame with its origin at the reference point in the circular orbit (the satellite station). The x axis is radially outward, the y axis is in the orbit plane in the direction of orbital motion, and the z axis is normal to the orbit plane. In this context the linear range is a sphere centered at the origin of the CW frame. However, as discovered by Gobetz,[12] the linear range can be extended to be a torus about the reference orbit by simply interpreting the components as cylindrical rather than Cartesian coordinates. The variable x then becomes a differential radius and y a differential longitude, with the form of the equations of motion being unchanged.

In first-order form, the CW equations of relative motion can be expressed in terms of a state vector $\boldsymbol{x}^T = [\boldsymbol{r}^T\ \boldsymbol{v}^T] = [x\ y\ z\ \dot{x}\ \dot{y}\ \dot{z}]$ as

$$\dot{\boldsymbol{x}} = \begin{bmatrix} \boldsymbol{O} & \boldsymbol{I} \\ \boldsymbol{A} & \boldsymbol{B} \end{bmatrix} \boldsymbol{x} \tag{1}$$

where $\boldsymbol{O}$ and $\boldsymbol{I}$ are the 3×3 zero and identity matrices, and

$$\boldsymbol{A} = \begin{bmatrix} 3n^2 & 0 & 0 \\ 0 & 0 & 0 \\ 0 & 0 & -n^2 \end{bmatrix} \tag{2}$$

and

$$\boldsymbol{B} = \begin{bmatrix} 0 & 2n & 0 \\ -2n & 0 & 0 \\ 0 & 0 & 0 \end{bmatrix} \tag{3}$$

The variable n is the mean motion in the nominal circular reference orbit. In Eq. (1) the skew-symmetric matrix $\boldsymbol{B}$ [Eq. (3)] represents the gyroscopic damping due to the fact that the motion is described in a rotating coordinate frame.

As seen in Eqs. (1–3) the out-of-plane (z) motion is uncoupled from the in-plane (x-y) motion. The state transition matrix representing the solution to Eq. (1) can be expressed in terms of 3×3 partitions as

$$\Phi(t, s) = \begin{bmatrix} \boldsymbol{M}(t, s) & \boldsymbol{N}(t, s) \\ \boldsymbol{S}(t, s) & \boldsymbol{T}(t, s) \end{bmatrix} \tag{4}$$

with the elements of the partitions given in Appendix A.

Necessary Conditions for an Optimal Rendezvous

The impulsive evasive maneuver involves transferring the satellite from the origin of the CW coordinate frame to a safe intermediate radius $\boldsymbol{r}_m$ at a time t_m, followed by a return trajectory culminating in a rendezvous with the origin at the time of the final impulse t_f. The magnitude of $\boldsymbol{r}_m$ is constrained by $r_m \geq R$, where R is a specified radius of the threat sphere (Fig. 1), and the time is constrained by $t_m \leq T_R$. The direction of $\boldsymbol{r}_m$ may be specified or free to be optimized, and the time of the final impulse t_f may be constrained or free.

The optimal solution to the problem stated requires the determination of the times, locations, directions, and the number of thrust impulses that utilize the least fuel in satisfying the boundary conditions and constraints of the problem. The necessary conditions for an optimal solution are conveniently expressed in terms of the primer vector, which is the adjoint to the velocity vector, and was first introduced by Lawden[13] and extended by Lion and Handelsman.[14]

A brief description of the necessary conditions for an optimal impulsive solution without interior path constraints in a general gravity field appears in Ref. 3. For the special case of the CW equations the necessary conditions were derived by Jezewski[15] and are described in a modified form in Appendix B of this paper.

To summarize, the necessary conditions for an optimal impulsive solution with interior path constraints are

1) The primer vector $\boldsymbol{p}(t)$ satisfies the same differential equation as the relative position vector $\boldsymbol{r}(t)$ and must be continuous.

2) The primer vector magnitude $p \leq 1$ during the transfer with impulses occurring at those instants at which $p = 1$.

3) At an impulse time the primer vector is a unit vector in the optimal thrust direction.

The main difference in these necessary conditions compared with those of Lawden[13] for the case of no interior path constraints is that $\dot{\boldsymbol{p}}$ and hence the Hamiltonian need not be continuous everywhere.

As discussed in Appendix B, the differential change in cost of the nominal three-impulse evasion-plus-return trajectory, $J = \Delta v_o + \Delta v_m + \Delta v_f$, due to changes in the time of the initial impulse t_o, the time of the final impulse t_f, the midcourse impulse time t_m, and position $\boldsymbol{r}_m$, is given by Eq. (B13):

$$\mathrm{d}J = -\Delta v_o\, \dot{\boldsymbol{p}}_o^T \boldsymbol{p}_o\, \mathrm{d}t_o - \Delta v_f\, \dot{\boldsymbol{p}}_f^T \boldsymbol{p}_f\, \mathrm{d}t_f + (\dot{\boldsymbol{p}}_m^+ - \dot{\boldsymbol{p}}_m^-)^T\, \mathrm{d}\boldsymbol{r}_m + (H_m^+ - H_m^-)^T\, \mathrm{d}t_m \tag{5}$$

where H is the Hamiltonian function of Eq. (B9).

As in the rendezvous without interior path constraint application in Ref. 3, it is evident from Eq. (5) that at the specified initial time on an optimal solution it is necessary that

$$\dot{\boldsymbol{p}}_o^T \boldsymbol{p}_o \leq 0 \tag{6}$$

If condition (6) is not satisfied, Eq. (5) indicates that an initial coast before the first impulse will decrease the cost J by making $\mathrm{d}J < 0$. At the specified time of the final impulse it is necessary that

$$\dot{\boldsymbol{p}}_f^T \boldsymbol{p}_f \geq 0 \tag{7}$$

with the equality case corresponding to an optimal final-time-open solution. If the inequality is satisfied in Eq. (7), one has the constrained-final-time optimal solution because the cost can be decreased only by violating the final time constraint. However, if condition (7) is not satisfied, a final coast ($dt_f < 0$) will decrease the cost as seen in Eq. (5).

The cost gradients for $\boldsymbol{r}_m$ and t_m have different interpretations in the case of an interior point constraint than in Refs. 3, 14, and 15. If $\boldsymbol{r}_m$ is specified, then $d\boldsymbol{r}_m = \boldsymbol{0}$ in Eq. (5), and it is not necessary that $\dot{\boldsymbol{p}}$ be continuous at the midcourse impulse as it is in the unconstrained midcourse impulse case. Similarly, if t_m is specified, the Hamiltonian does not need to be continuous at the midcourse impulse.

If $\boldsymbol{r}_m$ and t_m are not specified, but governed by the inequality constraints $r_m \geq R$ and $t_m \leq T_R$, then the gradients of Eq. (5) determine the constrained optimal solutions. For example, if $H_m^+ - H_m^- < 0$ when $t_m = T_R$, then one has obtained the constrained optimum because the cost can be decreased only by increasing t_m, which violates the constraint $t_m \leq T_R$. Also, if $\boldsymbol{r}_m$ is only constrained in magnitude such that $r_m \leq R$, a point on the threat sphere of radius R at which the gradient vector $\dot{\boldsymbol{p}}_m^+ - \dot{\boldsymbol{p}}_m^-$ is parallel to $\boldsymbol{r}_m$ is a constrained optimum, because the cost can be decreased only by moving $\boldsymbol{r}_m$ inside the sphere, which violates the constraint.

Three-Impulse Solutions

The maneuver sequence in the general case requires three impulses: a first impulse to depart the orbit station and to attain the safe location at $\boldsymbol{r}_m$, a midcourse impulse at $\boldsymbol{r}_m$ to establish a trajectory that returns to the original orbit station, and a final impulse to rendezvous with the original station at the final time.

The state equations for this maneuver can be simply written using the facts that $\boldsymbol{r}_o = \boldsymbol{r}_f = \boldsymbol{0}$ and $\boldsymbol{v}_o^- = \boldsymbol{v}_f^+ = \boldsymbol{0}$ because the orbit station, and hence the original and final state, is the origin of the CW coordinate frame. For simplicity, let $K \equiv t_m - t_o$ and $L \equiv t_f - t_m$. In terms of the partitions of the state transition matrix of Eq. (4) and Appendix A,

$$\boldsymbol{r}_m = \boldsymbol{N}(K)\,\Delta\boldsymbol{v}_o \tag{8a}$$

$$\boldsymbol{v}_m^- = \boldsymbol{T}(K)\,\Delta\boldsymbol{v}_o \tag{8b}$$

where the fact has been used that the first velocity change $\Delta\boldsymbol{v}_o$ is equal to the velocity vector after the first impulse $\boldsymbol{v}_o^+$, because $\boldsymbol{v}_o^- = \boldsymbol{0}$.

Similarly,

$$\boldsymbol{r}_f = \boldsymbol{0} = \boldsymbol{M}(L)\boldsymbol{r}_m + \boldsymbol{N}(L)\,\boldsymbol{v}_m^+ \tag{9a}$$

$$\boldsymbol{v}_f^- = -\Delta\boldsymbol{v}_f = \boldsymbol{S}(L)\boldsymbol{r}_m + \boldsymbol{T}(L)\,\boldsymbol{v}_m^+ \tag{9b}$$

where the fact that $\boldsymbol{v}_m^+ = \boldsymbol{0}$ has been used.

The midcourse velocity change $\Delta\boldsymbol{v}_m$ is given by

$$\Delta\boldsymbol{v}_m = \boldsymbol{v}_m^+ - \boldsymbol{v}_m^- \tag{10}$$

Combining Eqs. (8–10), one can explicitly write the three velocity changes as

$$\Delta\boldsymbol{v}_o = \boldsymbol{N}^{-1}(K)\,\boldsymbol{r}_m \tag{11a}$$

$$\Delta\boldsymbol{v}_m = -[\,\boldsymbol{T}(K)\boldsymbol{N}^{-1}(K) + \boldsymbol{N}(L)\boldsymbol{M}(L)]\boldsymbol{r}_m \tag{11b}$$

$$\Delta\boldsymbol{v}_f = [\boldsymbol{T}(L)\,\boldsymbol{N}^{-1}(L)\boldsymbol{M}(L) - \boldsymbol{S}(L)]\,\boldsymbol{r}_m \tag{11c}$$

where, as mentioned previously, the time interval K and the midcourse radius magnitude r_m are constrained and the time interval L may be constrained or free. The inverse of the N partition is assumed to exist for the time intervals considered. Isolated singularities of the matrix N exist and are discussed in Appendix A.

The solutions for the primer vector and its derivative are obtained as in Refs. 3, 4, 14, and 15 by applying as boundary conditions the necessary conditions that at the impulse times the primer vector is a unit vector in the velocity change direction, $\boldsymbol{p}_k = \Delta\boldsymbol{v}_k/\Delta v_k$, and the fact that the primer vector is continuous across impulses. The $\boldsymbol{p}_o$, $\boldsymbol{p}_m$, and $\boldsymbol{p}_f$ are known from Eqs. (11), yielding

$$\boldsymbol{p}_m = \boldsymbol{M}(K)\boldsymbol{p}_o + \boldsymbol{N}(K)\,\dot{\boldsymbol{p}}_o \tag{12}$$

$$\dot{\boldsymbol{p}}_m^- = \boldsymbol{S}(K)\boldsymbol{p}_o + \boldsymbol{T}(K)\,\dot{\boldsymbol{p}}_o \tag{13}$$

and also

$$\boldsymbol{p}_f = \boldsymbol{M}(L)\boldsymbol{p}_m + \boldsymbol{N}(L)\,\dot{\boldsymbol{p}}_m^+ \tag{14}$$

$$\dot{\boldsymbol{p}}_f = \boldsymbol{S}(L)\boldsymbol{p}_m + \boldsymbol{T}(L)\,\dot{\boldsymbol{p}}_m^+ \tag{15}$$

From Eq. (12) one determines the initial primer rate in terms of the known $\boldsymbol{p}_o$ and $\boldsymbol{p}_m$ as

$$\dot{\boldsymbol{p}}_o = \boldsymbol{N}^{-1}(K)\,[\,\boldsymbol{p}_m - \boldsymbol{M}(K)\boldsymbol{p}_o] \tag{16}$$

Similarly, from Eq. (14) one determines the primer rate immediately after the midcourse impulse in terms of the known $\boldsymbol{p}_m$ and $\boldsymbol{p}_f$ as

$$\dot{\boldsymbol{p}}_m^+ = \boldsymbol{N}^{-1}(L)\,[\,\boldsymbol{p}_f - \boldsymbol{M}(L)\,\boldsymbol{p}_m] \tag{17}$$

Subtracting Eq. (13) from Eq. (17) yields the discontinuity in $\dot{\boldsymbol{p}}_m$ across the midcourse impulse and supplies the cost gradient for $\boldsymbol{r}_m$ in Eqs. (5) and (B9). In addition, the discontinuity in the Hamiltonian of Eq. (B9), which is the cost gradient for t_m in Eqs. (5) and (B15), is given by

$$H_m^+ - H_m^- = \dot{\boldsymbol{p}}_m^{-T}\boldsymbol{v}_m^- - \dot{\boldsymbol{p}}_m^{+T}\boldsymbol{v}_m^+ \tag{18}$$

where the primer rates and the velocity vectors are known.

Because the primer vector and its rate are known at the beginning of each segment of the trajectory, the primer vector can be propagated along each segment using the transition matrix. If the primer magnitude exceeds unity anywhere, improvements to the trajectory can be made by introducing either an initial coast, a final coast, an increase in the final time, or a midcourse impulse, as outlined in Ref. 14 and successfully applied in Refs. 3 and 4.

Free-Return Two-Impulse Solutions

In the course of iteratively converging to solutions to the nonlinear final-time-open problem of Ref. 5, Clifton noted that if the midcourse radius $\boldsymbol{r}_m$ was constrained in magnitude only, as t_f and $\boldsymbol{r}_m$ were changed based on the gradients of Eq. (5), the magnitude of the velocity change $\Delta\boldsymbol{v}_m$ tended to zero. This indicated that values of $\boldsymbol{r}_m$ exist for which a two-impulse solution coasts through $\boldsymbol{r}_m$ at time t_m and returns to the origin without a midcourse impulse. The fuel cost of this type of maneuver is very economical, because the only cost is to get to $\boldsymbol{r}_m$ within the allotted time and then to coast to and rendezvous with the origin.

The linear dynamic model utilized in this study provides an excellent basis for analyzing this phenomenon. As will be seen later, the values of $\boldsymbol{r}_m$ and the corresponding maneuver times are determined by solving an eigenvalue problem.

A free-return trajectory of this type is one for which $\Delta\boldsymbol{v}_m = \boldsymbol{0}$ in Eq. (11b) and which returns to the origin after some elapsed time τ. Combining Eqs. (8) and (9) with $\boldsymbol{v}_m^+ = \boldsymbol{v}_m^-$ results in

$$\boldsymbol{r}_f = \boldsymbol{0} = \boldsymbol{M}(L)\,\boldsymbol{N}(K)\Delta\boldsymbol{v}_o + \boldsymbol{N}(L)\boldsymbol{T}(K)\Delta\boldsymbol{v}_o = \boldsymbol{N}(\tau)\Delta\boldsymbol{v}_o \tag{19}$$

where $\tau \equiv L + K$.

Combining Eq. (19) with Eq. (8) for the evasion radius $\boldsymbol{r}_m$ yields

$$\boldsymbol{0} = N(\tau)N^{-1}(K)\boldsymbol{r}_m \equiv \boldsymbol{Q}\boldsymbol{r}_m \tag{20}$$

where the matrix $\boldsymbol{Q}$ is defined for future reference.The free-return evasion radii are then eigenvectors of the matrix $\boldsymbol{Q}$ according to Eq. (20). For a nonzero $\boldsymbol{r}_m$ to exist, the matrix $\boldsymbol{Q}$ must be singular, which can occur only if $N(\tau)$ is singular and $N^{-1}(K)$ exists, i.e., $N(K)$ is nonsingular. The desired value of $\boldsymbol{r}_m$ to satisfy Eq. (20) then lies in the null-space of the matrix $\boldsymbol{Q}$, which is either a line through the origin of the CW frame or, in the case of two zero eigenvalues, a plane containing the origin.

The singularities of $N(\tau)$ occur at values of τ equal to integer multiples of π (integer multiples of half the circular reference period) and at other isolated values as discussed in Appendix A.

For each value of the final time τ for which $N(\tau)$ is singular (and thus permits a free-return trajectory), specifying the evasion time automatically determines the value of the return time $L = \tau - K$. The next step is to determine the eigenvector(s) of $\boldsymbol{Q}$ corresponding to the zero eigenvalue(s) of $\boldsymbol{Q}$.

A simple way to do this is to determine the locus of $\boldsymbol{r}_m$ for all evasion times $0 \le K \le \tau$. This is simply the free-return trajectory itself and can be obtained by evaluating $\Delta \boldsymbol{v}_o$ from Eq. (19) along with $\boldsymbol{r}_m$ from Eq. (8). The various cases are now considered.

For a free-return trajectory with $\tau = (2m - 1)\pi$, $m = 1, 2, 3, \ldots$, one substitutes $N[(2m - 1)\pi]$ into Eq. (19) to yield

$$\begin{bmatrix} 0 & 4 & 0 \\ -4 & -3(2m-1) & 0 \\ 0 & 0 & 0 \end{bmatrix} \Delta \boldsymbol{v}_o = \boldsymbol{0} \tag{21}$$

which admits the purely out-of-plane solution

$$\Delta \boldsymbol{v}_o^T = [0 \;\; 0 \;\; \Delta v_o] \tag{22}$$

Substituting into Eq. (8) using Eq. (A3), one finds that

$$N(K) = \begin{bmatrix} \sin K & 2(1-\cos K) & 0 \\ -2(1-\cos K) & 4\sin K - 3K & 0 \\ 0 & 0 & \sin K \end{bmatrix} \tag{23}$$

yields the solution for the eigenvector as

$$\boldsymbol{r}_m^T = [0 \;\; 0 \;\; r_m] \tag{24}$$

The initial velocity change of Eq. (22) can then be evaluated as

$$\Delta \boldsymbol{v}_o = \boldsymbol{N}^{-1}\boldsymbol{r}_m = [0 \;\; 0 \;\; r_m \csc K] \tag{25}$$

which is valid for all K except for $\sin K = 0$.

The final velocity change is determined to be

$$\Delta v_f = \Delta v_o \tag{26}$$

The entire maneuver represents an odd multiple of one-half cycle of the undamped oscillator represented by Eqs. (1–3) for the cross-track (out-of-plane) motion:

$$\ddot{z} = -n^2 z \tag{27}$$

and thus the total cost is $\Delta v_{\text{tot}} = 2r_m \csc K$. The orbit of this free-return trajectory in an inertial frame is a circular orbit of the same radius as the reference orbit, inclined at an angle equal to $r_m \csc K$ radians.

For a free-return trajectory with $\tau = 2m\pi$, $m = 1, 2, 3, \ldots$, one substitutes $N(2m\pi)$ into Eq. (19) to yield

$$\begin{bmatrix} 0 & 0 & 0 \\ 0 & -6m\pi & 0 \\ 0 & 0 & 0 \end{bmatrix} \Delta \boldsymbol{v}_o = \boldsymbol{0} \tag{28}$$

which admits the solution

$$\Delta \boldsymbol{v}_o^T = [\Delta v_{o_x} \;\; 0 \;\; \Delta v_{o_z}] \tag{29}$$

Substituting Eq. (29) into Eq. (8a) yields the eigenvector

$$\boldsymbol{r}_m^T = [\sin K\,\Delta v_{o_x} - 2(1 - \cos K)\Delta v_{o_x} \;\; \sin K\,\Delta v_{o_z}] \tag{30}$$

This indicates that the $\boldsymbol{Q}$ matrix has two zero eigenvalues and therefore has a null-space that is a plane containing the origin. Any $\boldsymbol{r}_m$ vector in this plane provides a free-return trajectory. The optimal choice of the components of $\Delta \boldsymbol{v}_o$ are those that provide a given magnitude of $\boldsymbol{r}_m$ (say, unity) with minimum magnitude $\Delta \boldsymbol{v}_o$. This is a simple linear programming problem that can be solved by inspection. First, set the sum of the squares of the components of $\Delta \boldsymbol{v}_o$ equal to unity:

$$[\sin^2 K + 4(1 - \cos K)^2]\Delta v_{o_x}^2 + \sin^2 K \Delta v_{o_z}^2 = 1 \tag{31}$$

To minimize the quantity $\Delta v_{o_x}^2 + \Delta v_{o_z}^2$, it is obvious that, since both coefficients on the left-hand side of Eq. (31) are positive, the optimal choice is $\Delta v_{o_z}^2 = 0$, because it has the smaller coefficient and is therefore less efficient in achieving the sum equal to unity. (This assumes $\cos K \neq 0$, which has already been ruled out because $N(K)$ is singular for this value.) Thus the optimal $\boldsymbol{r}_m$ is strictly in track (in plane) with

$$\Delta \boldsymbol{v}_o^T = \boldsymbol{r}_m \{[(\cos K - 1)(3\cos K - 5)]^{-1/2}\; 0 \;\; 0\} \tag{32}$$

and $\Delta \boldsymbol{v}_f = -\Delta \boldsymbol{v}_o$ for a total fuel cost of

$$\Delta v_{\text{tot}} = 2r_m [(\cos K - 1)(3\cos K - 5)]^{-1/2} \tag{33}$$

The direction of the optimal eigenvector, corresponding to $\Delta v_{o_z} = 0$, in Eq. (30) depends on the specified value of K. The angle ϕ is given by

$$\tan\phi = \frac{-2(1-\cos K)}{\sin K} \tag{34}$$

Figure 2 displays the free-return trajectory for several eigenvector directions. The inertial orbit for this trajectory is an elliptic orbit that has the same period as the circular reference orbit. The elliptic orbit achieves either periapse or apoapse one-quarter period after departing the orbit station, depending on whether $\Delta \boldsymbol{v}_o$ is directed radially inward or outward.

For $\tau = 2.8135\pi$ (506.43 deg) $\equiv \tau^*$, the free-return trajectory is obtained by substituting $N(\tau^*)$, along with the conditions in Eq. (A6), into Eq. (19) to yield

$$\begin{bmatrix} \sin\tau^* & 3\tau^*\sin\tau^*/4 & 0 \\ -3\tau^*\sin\tau^*/4 & 4\sin\tau^* - 3\tau^* & 0 \\ 0 & 0 & \sin\tau^* \end{bmatrix} \Delta \boldsymbol{v}_o = \boldsymbol{0} \tag{35}$$

which has the solution

$$\Delta \boldsymbol{v}_o^T = [\alpha \;\; -1 \;\; 0]\Delta v_o \tag{36}$$

where $\alpha \equiv 3\tau^*/4 = 6.629$

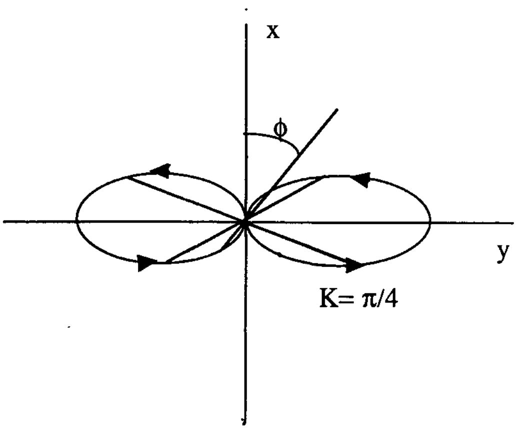

Fig. 2 Free-return trajectory for $\tau = 2m\pi$.

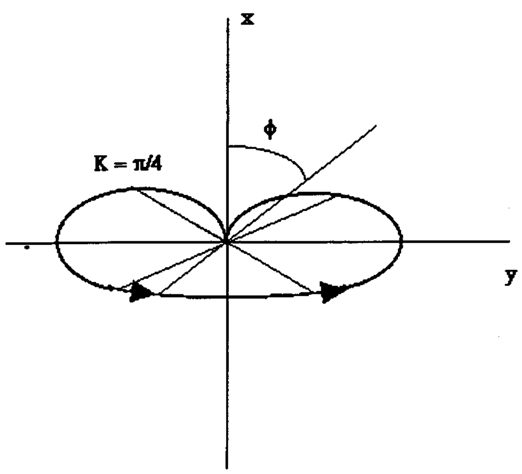

Fig. 3 Free-return trajectory for $\tau = 2.8135\pi$.

Substituting into Eq. (8) yields the eigenvectors

$$r_m = \begin{bmatrix} \alpha \sin K - 2(1 - \cos K) \\ 3K - 4 \sin K - 2\alpha(1 - \cos K) \\ 0 \end{bmatrix} \Delta v_o \tag{37}$$

The angle ϕ of the eigenvector with respect to the x axis is given by

$$\tan \phi = \frac{3K - 4 \sin K - 2\alpha(1 - \cos K)}{\alpha \sin K - 2(1 - \cos K)} \tag{38}$$

Figure 3 displays the free-return trajectory along with the various eigenvector directions, which correspond to different values of the evasion time K. The inertial orbit corresponding to this free-return trajectory is an elliptic orbit that has its periapse inside the reference orbit, apoapse outside the reference orbit, and period slightly different from the reference orbit. The return-on-station and rendezvous occur at the third crossing of the free-return orbit with the reference orbit. The other solutions mentioned in Appendix A, such as $T = 4.8906\pi$, correspond to the fifth and higher intersections of similar free-return trajectories.

The final velocity change is given by

$$\Delta v_f^T = [\alpha \;\; 1 \;\; 0] \Delta v_o \tag{39}$$

such that $\Delta v_f = \Delta v_o$, and from Eq. (8a) it follows that $\Delta v_o = r_m/w$ and the total fuel cost is

$$\Delta v_{\text{tot}} = \frac{2r_m}{w} \tag{40}$$

where

$$w \equiv \{[\alpha \sin K - 2(1 - \cos K)]^2 + [3K - 4 \sin K - 2\alpha(1 - \cos K)]^2\}^{1/2}$$

Details of Pure Cross-Track Free-Return Trajectory

As a specific example, the details of the primer vector for a pure cross-track free-return trajectory with $\tau = \pi$ are presented.The cross-track case is particularly easy to demonstrate because the transition matrix for the state $x^T = [z \;\; \dot{z}]$ is the simple rotation matrix given by the cross-track portion of Eq. (A1) as

$$\Phi(\theta) = \begin{bmatrix} \cos\theta & \sin\theta \\ -\sin\theta & \cos\theta \end{bmatrix} \tag{41}$$

where $\theta \equiv t - s$ (Appendix A).

Because the problem is one dimensional, the primer vector can be interpreted as a scalar that can have both positive and negative values. Applying the necessary conditions that the initial and final primer magnitudes must be unity, along with the equality case of Eq. (7) for a final-time-open optimal solution that dictates that $\dot{p}_f = 0$ in this case, results in the following relationship between the initial and final primer vector and its rate. From

$$\begin{bmatrix} p_m^- \\ \dot{p}_m^- \end{bmatrix} = \Phi(K) \begin{bmatrix} p_o \\ \dot{p}_o \end{bmatrix}; \qquad \begin{bmatrix} p_m^+ \\ \dot{p}_m^+ \end{bmatrix} = \begin{bmatrix} p_m^- \\ \dot{p}_m^- \end{bmatrix} + \begin{bmatrix} 0 \\ \pi_m \end{bmatrix} \tag{42a}$$

$$\begin{bmatrix} p_f \\ \dot{p}_f \end{bmatrix} = \Phi(L) \begin{bmatrix} p_m^+ \\ \dot{p}_m^+ \end{bmatrix} = \Phi(L) \left\{ \Phi(K) \begin{bmatrix} 1 \\ \dot{p}_o \end{bmatrix} + \begin{bmatrix} 0 \\ \pi_m \end{bmatrix} \right\} = \begin{bmatrix} I \\ 0 \end{bmatrix} \tag{42b}$$

where π_m represents the discontinuity in the variable $\dot{p}_m$. Simplifying, using $\Phi(L)\Phi(K) = \Phi(\tau) = \Phi(\pi)$ from Eq. (41).

$$\begin{bmatrix} -1 \\ -\dot{p}_o \end{bmatrix} + \begin{bmatrix} \sin L \\ \cos L \end{bmatrix} \pi_m = \begin{bmatrix} 1 \\ 0 \end{bmatrix} \tag{43}$$

which has the solution

$$\pi_m = 2 \csc L = 2 \csc K \tag{44a}$$

$$\dot{p}_o = 2 \cot L = -2 \cot K \tag{44b}$$

where $K = \pi - L$ has been used.

Figure 4 shows a phase-plane plot of the primer and its derivative for the case $K = \pi/4$. For this case $\dot{p}_o = -2$ and $\pi_m = 2\sqrt{2}$ from Eq. (44). As can be seen in Fig. 4, $p \leq 1$ throughout the solution, which is an additional necessary condition for an optimal solution. Note also that $p_m \neq 1$ as would be the case if a midcourse impulse were required.

Concerning the inequality constraints on evasion time and radius magnitude, one can examine the gradients in Eq. (5) to determine whether a constrained optimal solution has been obtained. The fact that the discontinuity in $\dot{p}_m$, represented by π_m, is positive indicates that the constrained optimal solution for $r_m \geq R$ is attained at $r_m = R$, because the cost can be reduced only by decreasing r_m, which violates the constraint. Similarly, the gradient for the evasion time is, from Eq. (B8), for the free-return case,

$$H_m^+ - H_m^- = -p_m^T v_m \tag{45}$$

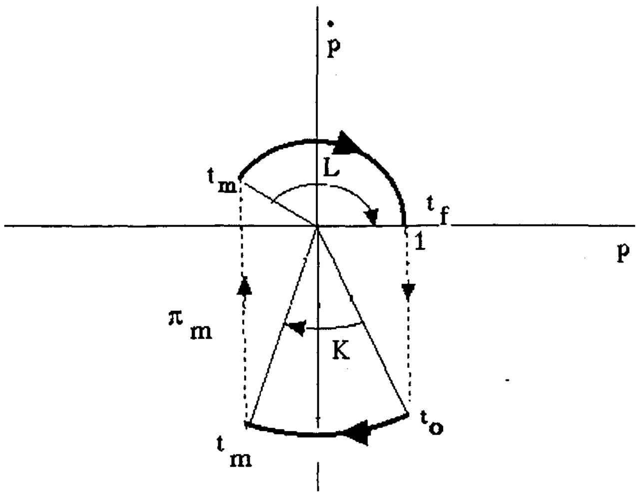

Fig. 4 Phase-plane plot for pure cross-track evasion.

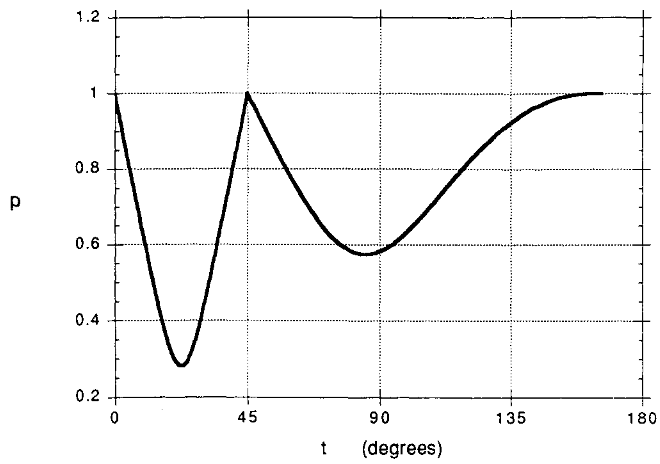

Fig. 6 Primer vector magnitude for optimal time-free case.

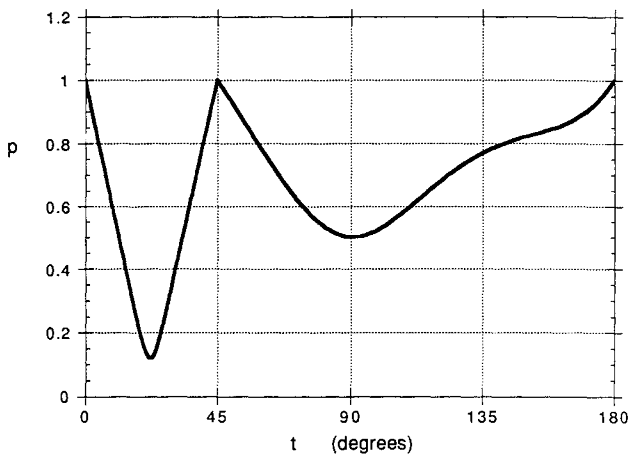

Fig. 5 Primer vector magnitude for optimal time-fixed case.

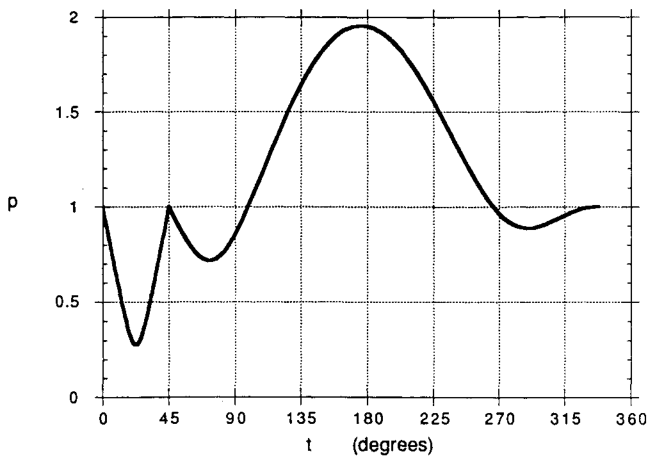

Fig. 7 Primer vector magnitude for nonoptimal time-free case.

which for the pure cross-track case is, since $v_m = T(K)\,\Delta v_o$ and $T(K) = \cos K$ from Eq. (41),

$$H_m^+ - H_m^- = -\pi_m v_m = -\pi_m \Delta v_o \cos K \tag{46}$$

which is negative for $\pi_m > 0$ and $0 < K < \pi/2$. This indicates that the cost can be reduced only by increasing the evasion time. Because the constraint is $t_m \leq T_R$, this implies that the constrained optimal solution is $t_m = T_R$.

Numerical Results

A few specific numerical examples of the trajectories discussed in the previous three sections are presented here.

For the pure cross-track free-return trajectory for $\tau = \pi$ and $K = \pi/4$, Eqs. (25) and (26) yield a total fuel cost of $2\sqrt{2}$ canonical velocity units per distance unit of r_m. For a geosynchronous orbit the canonical distance unit is 42,164 km and the time unit is 3.8 h, resulting in a velocity unit of 3.08 km/s. For a magnitude of r_m equal to 185 km (100 n.mi.) the total fuel cost is 38.26 m/s (125.3 ft/s). The value of $K = \pi/4$ for the geosynchronous case corresponds to an evasion time of approximately 3 h.

Figure 5 displays the primer vector magnitude p for the case $K = \pi/4$, $\tau = \pi$ (the total maneuver time is one-half the reference orbit period), and an in-track $\boldsymbol{r}_m^T = [0\ \ 1\ \ 0]$. The solution satisfies the necessary condition for an optimal solution that $p \leq 1$. In addition, the expected discontinuity in the time derivative of the primer vector occurs at time K. However, one must examine the various constraints to determine if a constrained optimal solution has been obtained.

The fact that the slope of the primer vector magnitude at the final time is positive satisfies the necessary condition in Eq. (7). Also, the fact that the cost gradient with respect to t_m in Eq. (5) has a negative value of -3.1 indicates a constrained optimal solution for $t_m \leq T_R = \pi/4$, because the cost can be lowered only by having t_m exceed T_R. Similarly, the cost gradient with respect to $\boldsymbol{r}_m$ in Eq. (5) is at an angle of 20.4 deg with $\boldsymbol{r}_m$ itself. If $\boldsymbol{r}_m$ is at its minimum magnitude (i.e., on the surface of the threat sphere), this indicates that for the specified evasion vector direction one has achieved the constrained optimal solution because the cost can be decreased only by going inside the threat sphere and violating the constraint. The fact that the cost gradient with respect to $\boldsymbol{r}_m$ is not parallel to $\boldsymbol{r}_m$ indicates that the optimal direction of $\boldsymbol{r}_m$ has not been achieved. One can move along the surface of the threat sphere and decrease the cost until the gradient and $\boldsymbol{r}_m$ become parallel. This is precisely the two-impulse free-return case where the magnitude of the impulse on the sphere goes to zero.

The primer history in Fig. 6 corresponds to an optimized final time case in which the equality condition is satisfied in Eq. (7). A one-dimensional search using the final-time gradient from Eq. (5) was utilized to converge iteratively on the optimal final time of 166 deg in this example case (11.04 h for geosynchronous orbit). The specified evasion direction is $\boldsymbol{r}_m^T = [0\ \ \sqrt{2}\ \ \sqrt{2}\,]/2$ and $K = \pi/4 = 45$ deg. The fuel cost is 3.20 per unit of r_m in canonical units, corresponding to 43.2 m/s (141.7 ft/s) for r_m equal to 185 km.

Lastly, Fig. 7 shows another local minimum for the same r_m and K as in Fig. 6. In this case the optimal final time is 337.9 deg. Note, however, that the necessary condition that $p \leq 1$ is violated on the return portion of the trajectory. The specific form of the primer magnitude violation in Fig. 7 indicates that an additional midcourse (fourth) impulse will lower the cost. This is a topic of ongoing research that utilizes the same procedure successfully applied in Ref. 3, which uses midcourse impulse gradients analogous to those in Eq. (5). The utility of the fourth impulse is demonstrated by the fact that the cost of the nonoptimal trajectory in Fig. 7 is already less than the local optimal solution shown in Fig. 6, namely, 42.5 m/s (139.5 ft/s).

Concluding Remarks

The combination of a linear dynamic model and primer vector theory has provided analytical results for the optimal impulsive satellite evasive maneuver problem. The return-on-station maneuvers are probably the most expensive in terms of fuel required, compared with other less-exacting maneuvers, but when optimized, they provide benchmarks with which costs of other maneuvers can be compared. Furthermore, the existence of four-impulse optimal trajectories has been demonstrated.

Appendix A: State Transition Matrix

The partitions of the state transition matrix of Eq. (4) are

$$\Phi(t, s) = \begin{bmatrix} M(t, s) & N(t, s) \\ S(t, s) & T(t, s) \end{bmatrix} \tag{A1}$$

where the individual elements are expressed in terms of $\theta \equiv t - s$ in canonical time units such that the reference orbit mean motion n is equal to unity as

$$M(\theta) = \begin{bmatrix} 4 - 3\cos\theta & 0 & 0 \\ 6(\sin\theta - \theta) & 1 & 0 \\ 0 & 0 & \cos\theta \end{bmatrix} \tag{A2}$$

$$N(\theta) = \begin{bmatrix} \sin\theta & 2(1-\cos\theta) & 0 \\ -2(1-\cos\theta) & 4\sin\theta - 3\theta & 0 \\ 0 & 0 & \sin\theta \end{bmatrix} \tag{A3}$$

$$S(\theta) = \begin{bmatrix} 3\sin\theta & 0 & 0 \\ -6(1-\cos\theta) & 0 & 0 \\ 0 & 0 & -\sin\theta \end{bmatrix} \tag{A4}$$

$$T(\theta) = \begin{bmatrix} \cos\theta & 2\sin\theta & 0 \\ -2\sin\theta & 4\cos\theta - 3 & 0 \\ 0 & 0 & \cos\theta \end{bmatrix} \tag{A5}$$

The singularities of the partition $N(\theta)$ are important because its inverse appears in expressions for the velocity changes, such as Eqs. (12–14) and elsewhere. Denoting the determinant of the matrix $N(\theta)$ by $D(\theta)$, from Eq. (A3):

$$D(\theta) = \sin\theta\,[8(1 - \cos\theta) - 3\,\theta\sin\theta] \tag{A6}$$

It is obvious that $D(m\pi) = 0$ for $m = 0, 1, 2, \ldots$, but other singularities also exist. This can be seen by writing Eq. (A6) as $D(\theta) = \sin\theta Z(\theta)$. Solutions to $Z = 0$ are then given by

$$\frac{1-\cos\theta}{\sin\theta} = \tan\frac{\theta}{2} = \frac{3\theta}{8} \tag{A7}$$

or, $\tan u = 3u/4$ where $u = \theta/2$.

Intersections of a straight line through the origin having slope less than unity with the tangent function occur on every branch of the tangent curve except the first.

The smallest two zeros of $Z(\theta)$ are determined numerically to be $2.8135\,\pi$ (506.43 deg) and $4.8906\,\pi$ (880.31 deg).

Appendix B: Cost Gradients

The CW equations of motion (1) can be written in equivalent form as

$$\dot{r} = v \tag{B1}$$

$$\dot{v} = Ar + Bv \tag{B2}$$

Corresponding to the state vector $x^T = [r^T \ v^T]$, one can define an adjoint vector $\lambda^T = [q^T \ p^T]$ as in Ref. 14, where p is the adjoint to the velocity vector (the primer vector) and q is the adjoint to the position vector. The state and adjoint equations of motion can be expressed in canonical form using the Hamiltonian function and Eq. (B1) as

$$H = p^T\dot{v} + q^T\dot{r} = p^T(Ar + Bv) + q^Tv \tag{B3}$$

$$\dot{r}^T = \frac{\partial H}{\partial q}, \qquad \dot{v}^T = \frac{\partial H}{\partial p} \tag{B4}$$

and

$$\dot{q}^T = -\frac{\partial H}{\partial r} = -p^TA \tag{B5}$$

$$\dot{p}^T = -\frac{\partial H}{\partial v} = -p^TB - q^T \tag{B6}$$

Combining the latter two equations and using the fact that the matrix A is symmetric and $\mathbf{B}$ is skew symmetric result in

$$\ddot{p} = Ap + B\dot{p} \tag{B7}$$

Comparing Eqs. (B7) with Eqs. (B1) and (B2), it is evident that the primer vector satisfies the same differential equation as the relative position vector r. Thus the state transition matrix $\Phi(t, s)$ of Appendix A can be used to propagate the vector composed of the primer vector and its derivative:

$$\begin{bmatrix} p(t) \\ \dot{p}(t) \end{bmatrix} = \Phi(t, s)\begin{bmatrix} p(s) \\ \dot{p}(s) \end{bmatrix} \tag{B8}$$

This property in the CW rotating coordinate frame is analogous to the inertial frame.[14] It thereby eliminates the need to use a separate transition matrix for the adjoint system to propagate the λ vector as was done in Ref. 15.

The Hamiltonian function (B3) can also be written in terms of p and $\dot{p}$ rather than p and q as

$$H = p^TAr - \dot{p}^Tv \tag{B9}$$

Using this formulation, one finds that the CW cost gradients derived in Ref. 14 become identical to those derived earlier for an inertial reference frame in Ref. 13. The necessary conditions for a minimum cost J due to a change in the time of the initial impulse $\mathrm{d}t_o$, a change in the time of the final impulse $\mathrm{d}t_f$, and changes in the midcourse position $\mathrm{d}r_m$ and time $\mathrm{d}t_m$ are obtained from the cost

$$J = \Delta v_o + \Delta v_m + \Delta v_f \tag{B10}$$

in a manner similar to Refs. 14 and 15 to be

$$\mathrm{d}J = -\Delta v_o\,\dot{p}_o^Tp_o\,\mathrm{d}t_o - \Delta v_f\,\dot{p}_f^Tp_f\,\mathrm{d}t_f + (\dot{p}_m^+ - \dot{p}^-)^T\,\mathrm{d}r_m + (H_m^+ - H_m^-)\,\mathrm{d}t_m \tag{B11}$$

From the expression for dJ, using the continuity of $\boldsymbol{p}_m$, one identifies the gradients of the cost as

$$\frac{\partial J}{\partial t_o} = -\Delta v_o \dot{\boldsymbol{p}}_o^T \boldsymbol{p}_o \tag{B12}$$

$$\frac{\partial J}{\partial t_f} = -\Delta v_f \dot{\boldsymbol{p}}_f^T \boldsymbol{p}_f \tag{B13}$$

$$\frac{\partial J}{\partial \boldsymbol{r}_m} = (\dot{\boldsymbol{p}}_m^+ - \dot{\boldsymbol{p}}^-)^T \tag{B14}$$

$$\frac{\partial J}{\partial t_m} = (H_m^+ - H_m^-) \tag{B15}$$

These cost gradients are used to perform the iterative cost optimization and provide convergence.

References

[1]Kelley, H. J., Cliff, E. M., and Lutze, F. H., "Pursuit/Evasion in Orbit," *Journal of the Astronautical Sciences,* Vol. 29, No. 3, 1981, pp. 277–288.

[2]Kelley, H. J., Cliff, E. M., and Lutze, F. H., "Orbital-Maneuver–Sequence Optimization," USAF Report AFRPL TR-85-090, Dec. 1985.

[3]Prussing, J. E., and Chiu, J.-H., "Optimal Multiple-Impulse Time-Fixed Rendezvous Between Circular Orbits," *Journal of Guidance, Control, and Dynamics,* Vol. 9, No. 1, 1986, pp. 17–22.

[4]Prussing, J. E., Wellnitz, L. W., and Heckathorn, W. G., "Optimal Impulsive Time-Fixed Direct-Ascent Interception," *Journal of Guidance, Control, and Dynamics,* Vol. 12, No. 4, 1989, pp. 487–494.

[5]Clifton, R. S., "Optimal Multiple-Impulse ASAT Avoidance Maneuvers," M.S. Thesis, Dept. of Aeronautical and Astronautical Engineering, Univ. of Illinois at Urbana-Champaign, Urbana, IL, 1987.

[6]Widhalm, J. W., and Eide, S. A., "Optimal Continuous Thrust In-Plane Orbital Evasive Maneuvers," AIAA 26th Aerospace Sciences Meeting, AIAA Paper 88-0374, Reno, NV, Jan 1988.

[7]Murphy, G. O., "Optimal Multiple-Impulse ASAT Interception," M.S. Thesis, Dept. of Aeronautical and Astronautical Engineering, Univ. of Illinois at Urbana-Champaign, Urbana, IL, 1988.

[8]Burk, R. V., and Widhalm, J. W., "Minimum Impulse Orbital Evasive Maneuvers," *Journal of Guidance, Control, and Dynamics,* Vol. 12, No. 1, 1989, pp. 121–123.

[9]Lembeck, C. A., and Prussing, J. E., "Optimal Impulsive Intercept with Low-Thrust Rendezvous Return," *Journal of Guidance, Control, and Dynamics,* Vol. 16, No. 3, 1993, pp. 426–433.

[10]Clohessy, W. H., and Wiltshire, R. S., "Terminal Guidance System for Satellite Rendezvous," *Journal of the Aerospace Sciences,* Vol. 27, 1960, p. 653.

[11]Prussing, J. E., and Conway, B. A., *Orbital Mechanics,* Oxford Univ. Press, New York, 1993.

[12]Gobetz, F. W., "Optimal Variable-Thrust Transfer of a Power-Limited Rocket Between Neighboring Circular Orbits," *AIAA Journal,* Vol. 2, No. 2, 1964, pp. 339–343.

[13]Lawden, D. F., *Optimal Trajectories for Space Navigation,* Butterworths, London, England, UK, 1963.

[14]Lion, P. M., and Handelsman, M., "The Primer Vector on Fixed-Time Impulsive Trajectories," *AIAA Journal,* Vol. 6, No. 1, 1968, pp. 127–132.

[15]Jezewski, D. J., "Primer Vector Theory Applied to the Linear Relative Motion Equation," *Optimal Control Applications and Methods,* Vol. 1, 1980, pp. 387–401.